

## **Investigation of the Cavitation Index of Bottom Outlets Equipped with a Sluice Gate**

Ahmet Baylar<sup>1\*</sup>, Alp Bugra Aydin<sup>2</sup>, Fahri Ozkan<sup>2</sup>

<sup>1</sup>Department of Civil Engineering, Eskisehir Technical University, Eskisehir, Turkey, abaylar@eskisehir.edu.tr

<sup>2</sup>Department of Civil Engineering, Firat University, Elazig, Turkey, baydin@firat.edu.tr, fozkan@firat.edu.tr

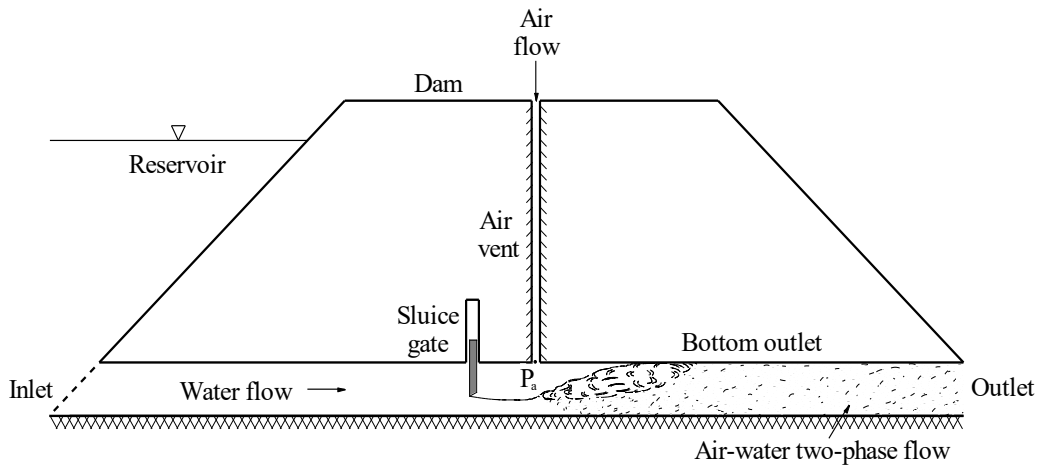
## Abstract

8 Cavitation, erosion, vibration, and crushing are the main causes of damage in hydraulic  
9 structures. Cavitation is a phenomenon that can damage hydraulic structures at high velocities.  
10 Cavitation occurs when the pressure in the water flow drops below the vapor pressure of the  
11 water. Flow aeration in hydraulic structures is known to reduce cavitation damage. Bottom  
12 outlet aeration is a particular instance of this. The high-velocity flow in the bottom outlet is a  
13 mixed air-water flow. The airflow results from the sub-atmospheric pressure downstream of the  
14 gate. The air entrained by the high-velocity flow is supplied by the air vent. If the air required  
15 by the flow is not supplied, the pressure drop downstream of the gate will cause cavitation. This  
16 study investigates the cavitation index of bottom outlets equipped with a sluice gate using three  
17 different bottom outlet cross-sections. Results indicate that the cavitation index decreased with  
18 increasing Froude number. The bottom outlet cross-sectional geometry did not have a big effect  
19 on the cavitation index. It is also presented a formula for estimating the cavitation index, which  
20 relates the cavitation index to the Froude number, the gate opening rate, and the ratio of the  
21 hydraulic radius to the bottom outlet length.

**Keywords:** Air-water flow, bottom outlet, cavitation, hydraulic structures, sluice gate

24 1. Introduction

Bottom outlets serve a variety of functions in large dams, including providing an emergency spillway for the reservoir, regulating the water level in the reservoir, and preventing sediment accumulation at the base of the dam. They are hydraulic structures that contain a high-velocity air-water flow. A high-velocity, low-pressure flow occurs downstream of a gate that partially closes the cross-sectional area of the bottom outlet. Because of this high-velocity flow, pressures lower than atmospheric can occur in the bottom outlet. These pressures could theoretically be as low as the vapor pressure of water. When connected to the atmosphere with a vent downstream of the gate, air is drawn into the vent as shown in Figure 1. The reduction in pressure downstream of the gate relative to atmospheric pressure depends on the degree of the gate opening.



35

36 **Figure 1.** High-velocity, low-pressure flow in a bottom outlet

37

38 The main problem with bottom outlets is cavitation phenomena, particularly after the flow  
 39 control gates, which occur at different gate opening rates due to the high flow velocity and  
 40 pressure drop downstream of the gates. Cavitation occurs whenever the pressure in the flow of  
 41 water drops to the value of the pressure of the saturated water vapor,  $P_v$  (at the prevailing  
 42 temperature); cavities filled by vapor, and partly by gases excluded from the water as a result  
 43 of the low pressure, are formed. When these bubbles are carried by the flow into regions of  
 44 higher pressure, the vapor rapidly condenses and the bubbles implode, the cavities being  
 45 suddenly filled by the surrounding water. Not only is this process noisy, with disruption in the  
 46 flow pattern, but - more importantly - if the cavity implodes against a surface, the violent impact  
 47 of the water particles acting in rapid succession at very high pressures (of the order of 1000  
 48 atm), if sustained over some time, causes significant damage to the (concrete or steel) surface,  
 49 which can lead to a complete failure of the structure. Cavitation corrosion (pitting) and the  
 50 often-associated vibration is therefore a phenomenon that needs to be considered in the design  
 51 of hydraulic structures and prevented whenever possible (Novak et al, 2007).

52

53 The presence of cavitation in a high-velocity bottom outlet introduces a critical condition that  
 54 can cause damage. Chanson (2000) recommended that cavitation damage can occur when the  
 55 velocity exceeds 12 m/s in clear water. For a given flow characteristic, the cavitation index also  
 56 indicates whether a structure is susceptible to cavitation. It is a dimensionless parameter defined  
 57 by Equation (1). Falvey (1990) suggested that the critical value of the cavitation index is about  
 58 0.2. If the cavitation index is less than this critical value, surface damage should be expected.

59

60 Many studies have been carried out on cavitation in hydraulic structures. Falvey HT (1983)  
61 presented several criteria to prevent cavitation damage to the flow surface based on the  
62 cavitation index. May (1987) reviewed the literature on cavitation in large hydraulic structures  
63 to summarize the current state of knowledge, provide guidance to designers, and identify areas  
64 requiring further research. Falvey (1990) developed equations to calculate the cavitation index.  
65 Lee & Hoopes (1996), Wahl et al. (2019) and Wahl & Falvey (2022) developed a model to  
66 predict the occurrence of cavitation damage using factors that influence the phenomenon:  
67 cavitation index, velocity, air concentration, material resistance, and time of exposure to flow.  
68 Dong and Su (2006) found that aerators can increase the pressure in the cavitation region,  
69 reducing the risk of cavitation damage to the spillway. Matos et al. (2022) analysed minimum  
70 extreme pressures in stepped spillways considering different ranges of specific discharges,  
71 chutes with a slope, and step widths. The results indicated that maximum unit discharges of  
72 about 15-20 m<sup>3</sup>/s are considered advisable on 53° sloping large-stepped spillways without  
73 artificial aeration, for step heights ranging from 0.6 to 1.2 m. For much higher unit discharges,  
74 a considerable reach of the spillway may potentially be prone to the risk of cavitation damage.

75

76 In a bottom outlet, an air vent is usually installed immediately downstream of the gate to provide  
77 sufficient air to flow. Previous studies have shown that injecting air into the flow downstream  
78 of the gate can significantly reduce the risk of cavitation damage. Numerous studies have been  
79 reported on the air-demand ratio ( $Q_a/Q_w$ ) in bottom outlets - e.g., Aydin et al. (2021, 2022,  
80 2024a, 2024b), Baylar and Batan (2010), Baylar et al. (2010, 2021, 2022), Campbell and  
81 Guyton (1953), Escarameia (2007), Haindl and Sotornik (1957), Hohermuth (2019),  
82 Hohermuth et al. (2020), Kalinske and Robertson (1943), Mortensen (2009), Mortensen et al.  
83 (2011, 2012), Mortensen and Kubitschek (2016), Oveson (2008), Ozkan et al. (2006a, 2006b,  
84 2010, 2014, 2015), Pengchengi et al. (2022), Sharma (1976), Speerli (1999), Speerli and Hager  
85 (2000), Stahl and Hager (1999), Tullis and Larchar (2011), Tuna et al. (2014), Unsal et al.  
86 (2008, 2009, 2014), and USACE (1964). These studies indicate that the air-demand ratio for  
87 bottom outlets is a function of hydraulic and geometric parameters and, for a given geometry,  
88 depends mainly on the flow types. Based on experimental data and theoretical studies, the  
89 authors have developed some equations to determine the air-demand ratio under different flow  
90 patterns.

91

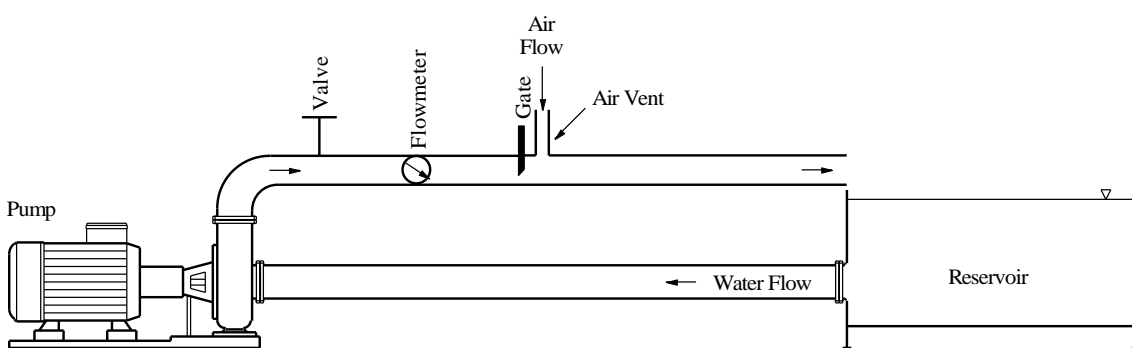
92 There has been no detailed study of the effect of cross-sectional geometry on the cavitation  
93 index of sluice-gated bottom outlets. Based on this information, this study investigated the  
94 effect of cross-sectional geometry on the cavitation index of sluice-gated bottom outlets.

95

## 96 **2. Experimental**

97 The experiments were carried out using an experimental apparatus at the Hydraulic Laboratory  
98 of the Faculty of Engineering, Firat University, Elazig, Turkey. The experimental setup used to  
99 measure the air inlet velocity is shown in Fig. 2. The water in the reservoir was pumped to the  
100 pipe by a vacuum pump. The flow rate was adjusted by a flow control valve. A calibrated  
101 electromagnetic flowmeter was used to measure the flow rates.

102



103

104 **Figure 2.** Schematic of experimental setup

105

106 Three different bottom outlet cross-sections were used to study the effect of cross-section  
107 geometry on the cavitation index. Rectangular bottom outlets with dimensions of width: 60 mm  
108 × height: 100 mm and width: 100 mm × height: 60 mm were selected to have the same cross-  
109 sectional area as a 3-inch diameter circular bottom outlet. 168 experiments were conducted for  
110 the 60 × 100 rectangular bottom outlet, 168 experiments were conducted for the 100 × 60  
111 rectangular bottom outlet, and 168 experiments were conducted for the circular bottom outlet.

112

113 For all bottom outlet cross-sectional geometries, the gate opening rate, which refers to the ratio  
114 of the water flow cross-sectional area to the bottom outlet cross-sectional area, was selected as  
115 a percentage of 10, 15, 20, 30, 40, and 60. Bottom outlet lengths of 1, 2, 4, and 6 meters were  
116 used. A 200 mm high vent was placed downstream of the gate to entrain air into the bottom  
117 outlet. A Testo 435 anemometer was used to measure the air velocity in the vent. This  
118 measurement was made by placing the anemometer in the center of the vent. Air velocity  
119 measurements were taken for 60 seconds or longer. The accuracy of the anemometer was  $\pm(0.2$

120 m/s + 1.5% of mv). The verticality of the anemometer to the direction of flow in the vent was  
121 taken into account for accurate measurements.

122

123 In this study, the cavitation index was calculated by using Eq. 1.

124

$$\sigma = \frac{h_p + h_a - h_v}{V_w^2 / 2g} \quad (1)$$

125

126 where  $h_p$  is local water pressure in m of water,  $h_a$  is ambient pressure in m of water,  $h_v$  is  
127 saturated water vapor pressure in m of water,  $V_w$  is average clear-water flow velocity and  $g$  is  
128 gravitational acceleration.

129

130 Air pressure can be calculated by applying the Bernoulli equation to the air vent.

131

$$\frac{P_a}{\rho_a g} = -(1 + \xi) \frac{V_a^2}{2g} \quad (2)$$

132

133 where  $P_a$  is relative air pressure,  $\rho_a$  is air density,  $g$  is gravitational acceleration,  $\xi$  is total loss  
134 coefficient of air vent and  $V_a$  is air velocity in air vent.

135

136 The total loss coefficient of the air vent is equal to the sum of the local fluid resistance  
137 coefficient ( $\xi_{loc}$ ) and the frictional resistance coefficient of the air vent length ( $\xi_{fr}$ ).

138

$$\xi = \xi_{loc} + \xi_{fr} \quad (3)$$

139

140 The local fluid resistance coefficient is due to a sudden change in the cross-sectional area of the  
141 airflow (sudden increase). The frictional resistance coefficient of the air vent length is calculated  
142 from the following equation.

143

$$\xi_{fr} = \lambda \frac{L_0}{D_0} \quad (4)$$

144

145 where  $\lambda$  is friction coefficient, which can be determined from the Moody diagram,  $L_0$  is length  
146 of air vent and  $D_0$  is diameter of air vent.

147

148 The cavitation index is a function of the following variables:

149

$$\sigma = f_1 (V_w, g, h_e, \varphi) \quad (5)$$

150

151 Using dimensional analysis, the most effective parameters for cavitation index in bottom  
152 outlets are derived as:

153

$$\sigma = f_2 (V_w / \sqrt{g h_e}, \varphi) \quad (6)$$

154

$$\sigma = f_3 (Fr, \varphi) \quad (7)$$

155

156 where  $\sigma$  is cavitation index,  $V_w$  is water velocity under gate,  $g$  is gravitational acceleration,  $h_e$   
157 is effective depth (ratio of water flow cross-sectional area to water surface width), and  $\varphi$  is ratio  
158 of water cross-sectional flow area to bottom outlet cross-sectional area.

159

160 The Froude number was calculated from the effective depth rather than the depth at the vena  
161 contracta section. In literature, the Froude number has often been based on the vena contracta  
162 section. Since high-head gated bottom outlets involve high-velocity air-water mixture flow, in  
163 this study the Froude number was based on the effective depth in the bottom outlet to avoid the  
164 problem of determining flow depths and velocities at the vena contracta section.

165

### 166 **3. Results and Analysis**

167 The aim of this study was to determine the effect of bottom outlet cross-section geometry on  
168 the cavitation index. This objective was achieved by building a physical experimental setup,  
169 conducting experiments, obtaining data, analyzing the data, and presenting the results.

170

171 Figures 5-10 show plots of the cavitation index ( $\sigma$ ) versus the Froude number (Fr) of the bottom  
172 outlet cross-sectional geometry, gate opening rate ( $\varphi$ ), and bottom outlet length (L). It is seen  
173 that the cavitation index decreased for all bottom outlet cross-sectional geometries, gate opening  
174 rates, and bottom outlet lengths, as the Froude number increased. This indicates that there is an  
175 inverse relationship between the Froude number and the cavitation index.

176

177 As the Froude number increased, the cavitation index decreased rapidly for all bottom outlet  
178 cross-sectional geometries, gate opening rates, and bottom outlet lengths (Figures 5-10). It  
179 appears that Froude number 25 at 10% gate opening rates, Froude number 20 at 15% gate  
180 opening rates, Froude number 15 at 20% gate opening rates, Froude number 12 at 30% gate  
181 opening rates, Froude number 10 at 40% gate opening rates, and Froude number 8 at 60% gate  
182 opening rates showed negative values for the cavitation index. It was observed that there was  
183 no significant decrease in the cavitation index with a further increase in the Froude number after  
184 the points where the cavitation index went negative.

185

186 Following a detailed review of the experiments, it was observed that the cavitation index  
187 increased at low Froude numbers with the increase in the gate opening rate for all bottom outlet  
188 cross-sectional geometries and bottom outlet lengths. It was found that the cavitation index  
189 reached zero at lower Froude numbers as the gate opening rate increased. It was determined  
190 that there was no risk of cavitation for Froude numbers less than 20 at 10% gate opening rates,  
191 values of Froude numbers less than 15 at 15% gate opening rates, values of Froude numbers  
192 less than 13 at 20% gate opening rates, values of Froude numbers less than 11 at 30% gate  
193 opening rates, values of Froude numbers less than 10 at 40% gate opening rates and values of  
194 Froude numbers less than 9 at 60% gate opening rates. Furthermore, the change in cavitation  
195 index decreased as the gate opening rate increased for all bottom outlet cross-sectional  
196 geometries and bottom outlet lengths. The reason for this phenomenon appears to be that when  
197 the gate opening rate increased, the flow velocity below the gate decreased. This, in turn, led to  
198 a decrease in the pressure drop.

199

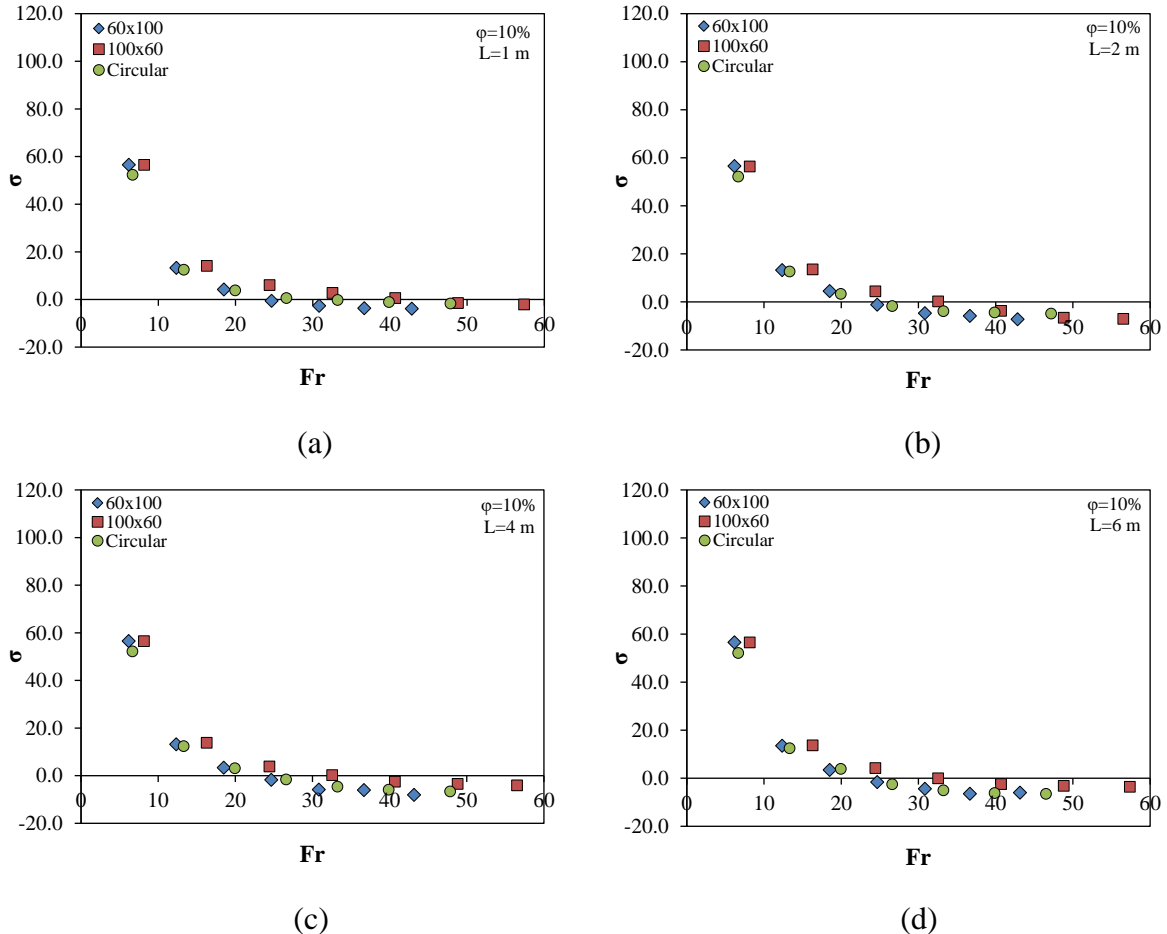
200 The  $100 \times 60$  rectangular cross-sectional bottom outlet generally exhibited a higher cavitation  
201 index for all gate opening rates and bottom outlet lengths. Conversely, the  $60 \times 100$  rectangular  
202 cross-sectional bottom outlet generally demonstrated a lower cavitation index for all gate  
203 opening rates and bottom outlet lengths. However, the effect of bottom outlet cross-sectional  
204 geometry on the cavitation index was not found to be significant for all gate opening rates and  
205 bottom outlet lengths.

206

207 Similarly, the bottom outlet length did not have a big effect on the cavitation index for all bottom  
208 outlet cross-sectional geometries and gate opening rates. At high Froude numbers, the cavitation  
209 index reached higher values at 6 m bottom outlet length for all bottom outlet cross-sectional

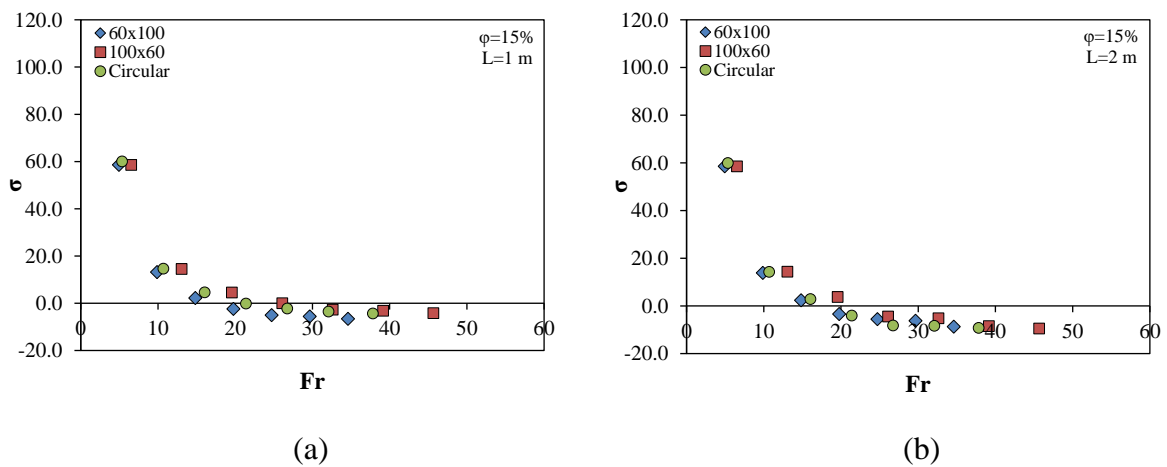
geometries and gate opening rates. At a 60% gate opening rate, the effect of bottom outlet length on the cavitation index was nearly negligible for all bottom outlet cross-sectional geometries.

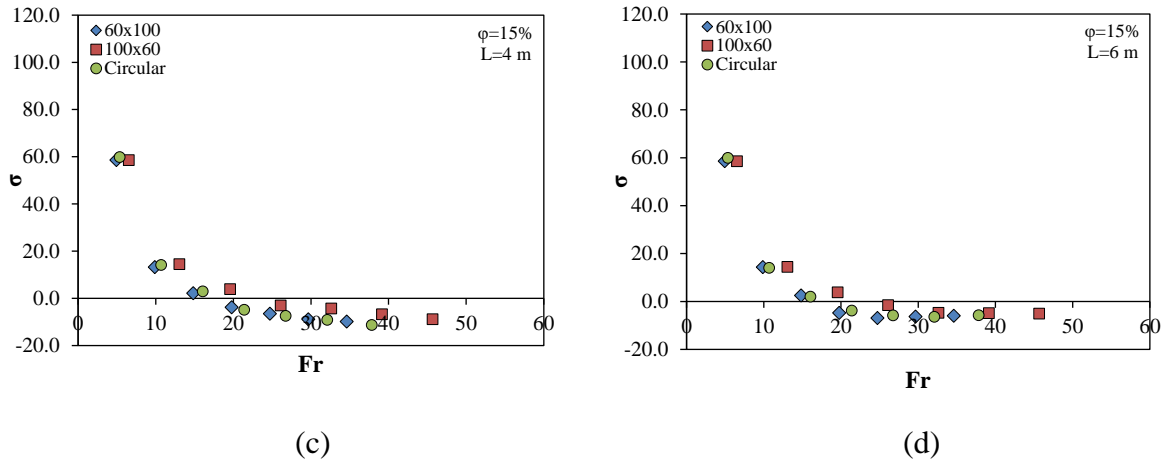
212



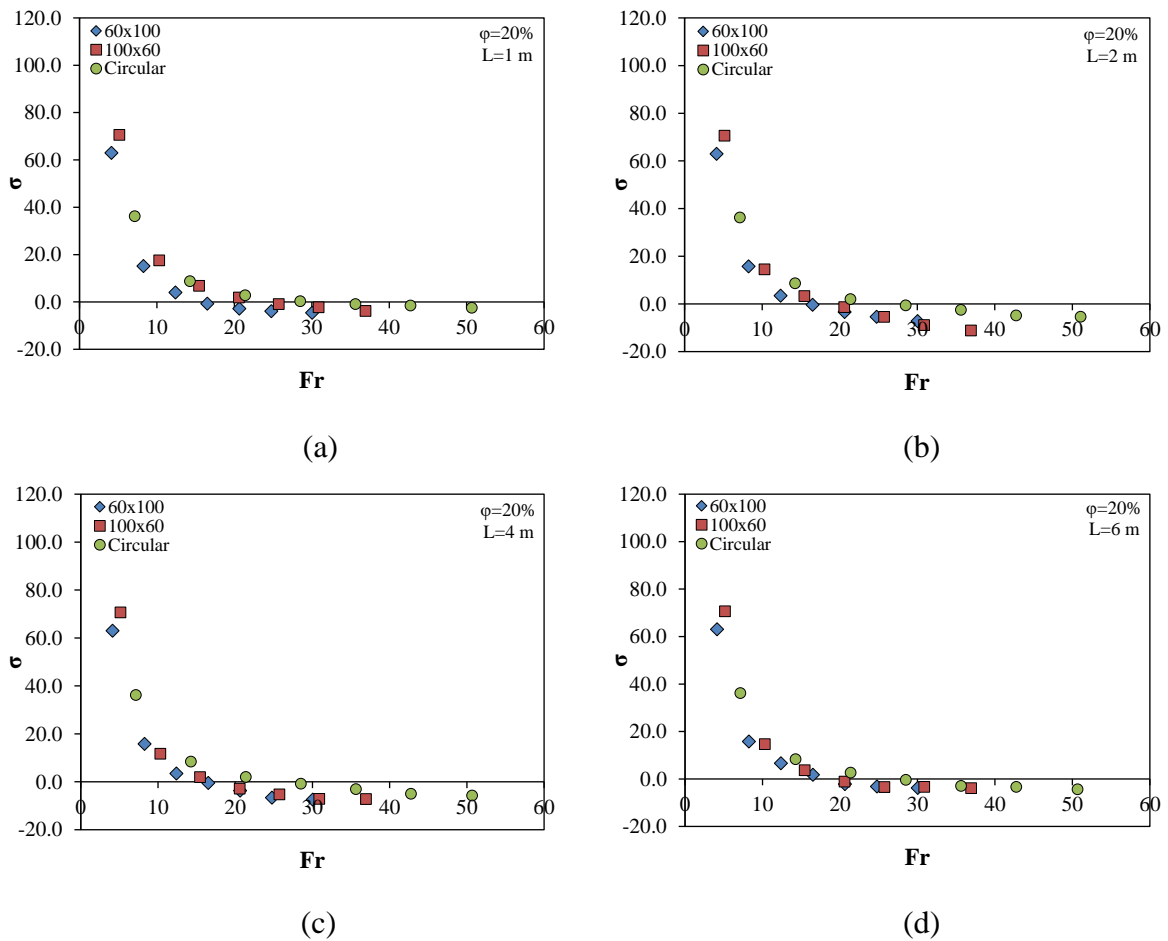
213 **Figure 5.** Variation of  $\sigma$  plotted against the Froude number for different bottom outlet lengths  
214 at  $\varphi=10\%$  (a)  $L=1\text{ m}$ , (b)  $L=2\text{ m}$ , (c)  $L=4\text{ m}$ , (d)  $L=6\text{ m}$

215

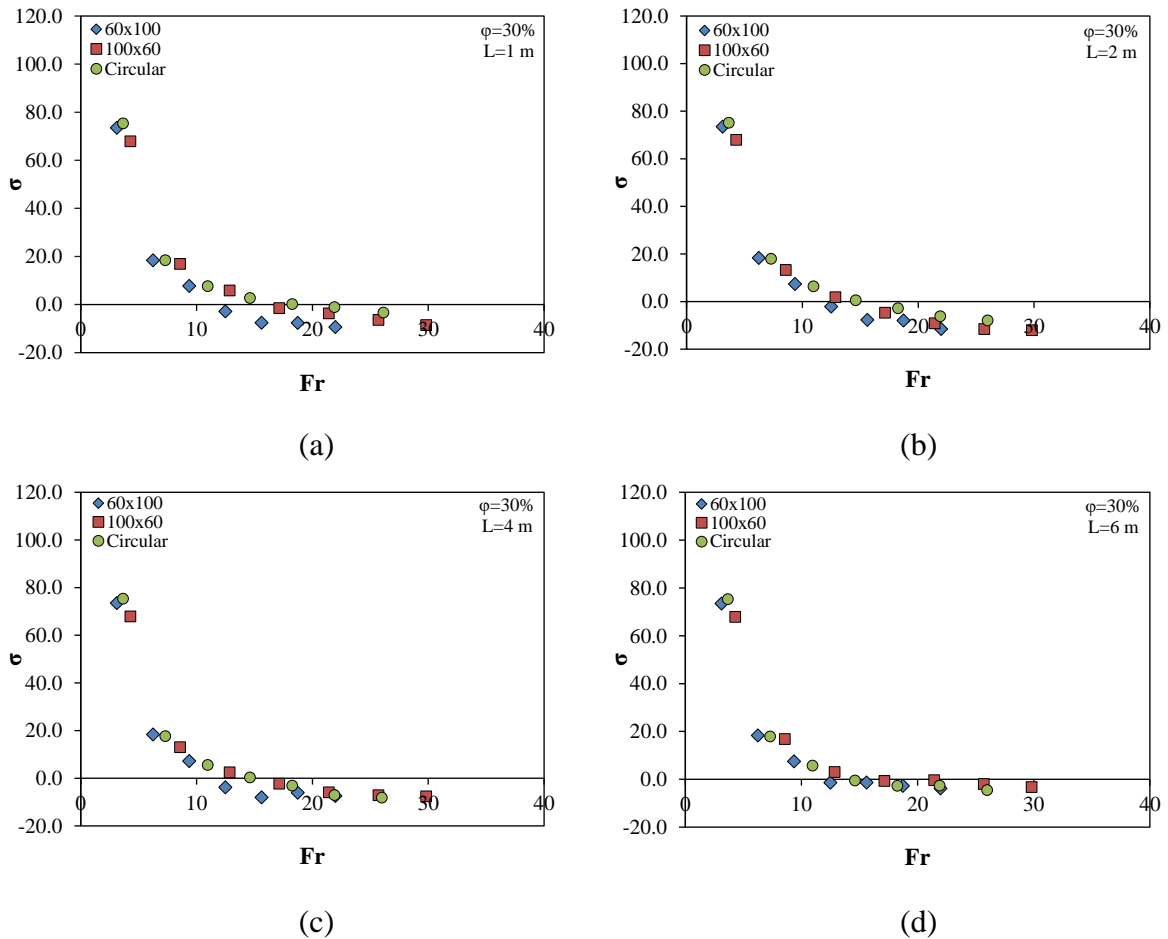




216 **Figure 6.** Variation of  $\sigma$  plotted against the Froude number for different bottom outlet lengths  
 217 at  $\varphi=15\%$  (a)  $L=1 \text{ m}$ , (b)  $L=2 \text{ m}$ , (c)  $L=4 \text{ m}$ , (d)  $L=6 \text{ m}$   
 218

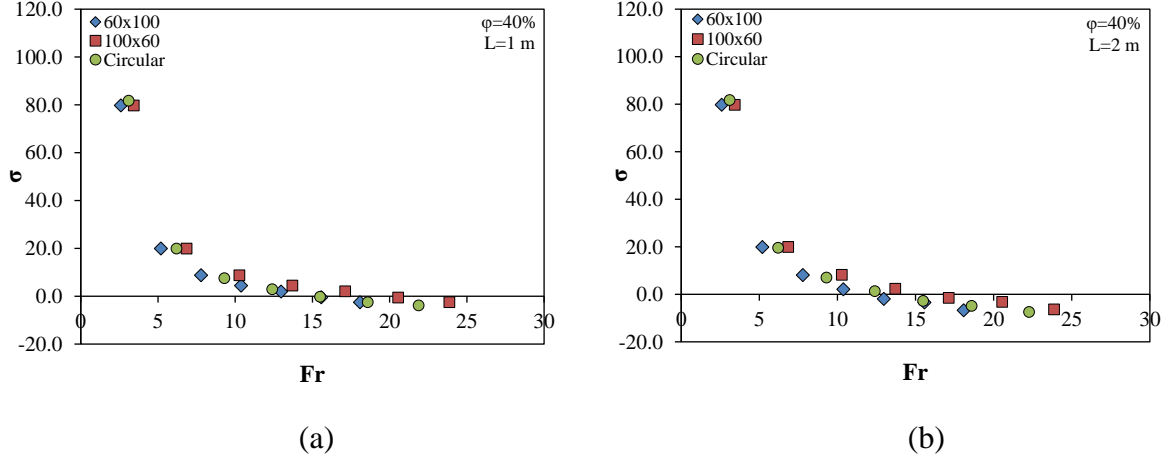


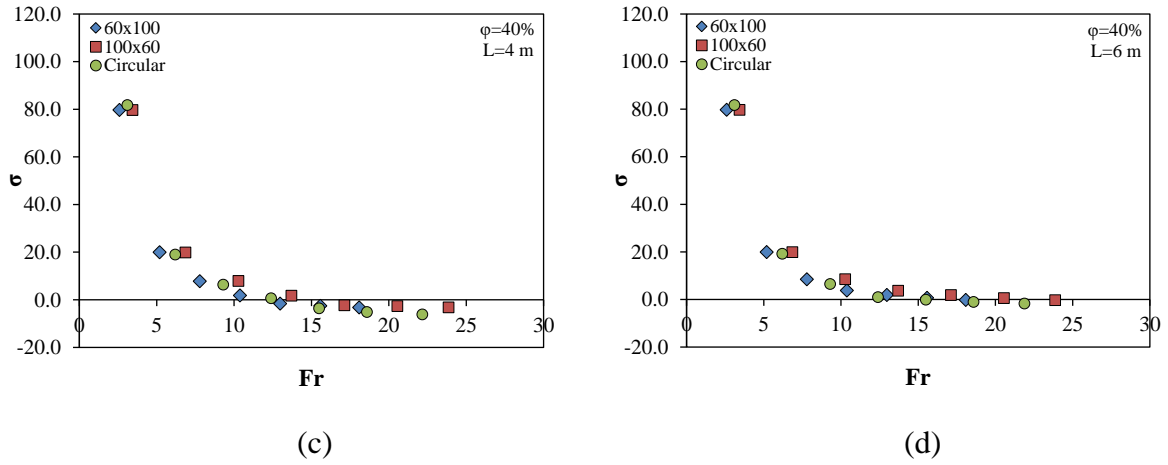
219 **Figure 7.** Variation of  $\sigma$  plotted against the Froude number for different bottom outlet lengths  
 220 at  $\varphi=20\%$  (a)  $L=1 \text{ m}$ , (b)  $L=2 \text{ m}$ , (c)  $L=4 \text{ m}$ , (d)  $L=6 \text{ m}$   
 221



222 **Figure 8.** Variation of  $\sigma$  plotted against the Froude number for different bottom outlet lengths  
223 at  $\varphi=30\%$  (a)  $L=1\text{ m}$ , (b)  $L=2\text{ m}$ , (c)  $L=4\text{ m}$ , (d)  $L=6\text{ m}$

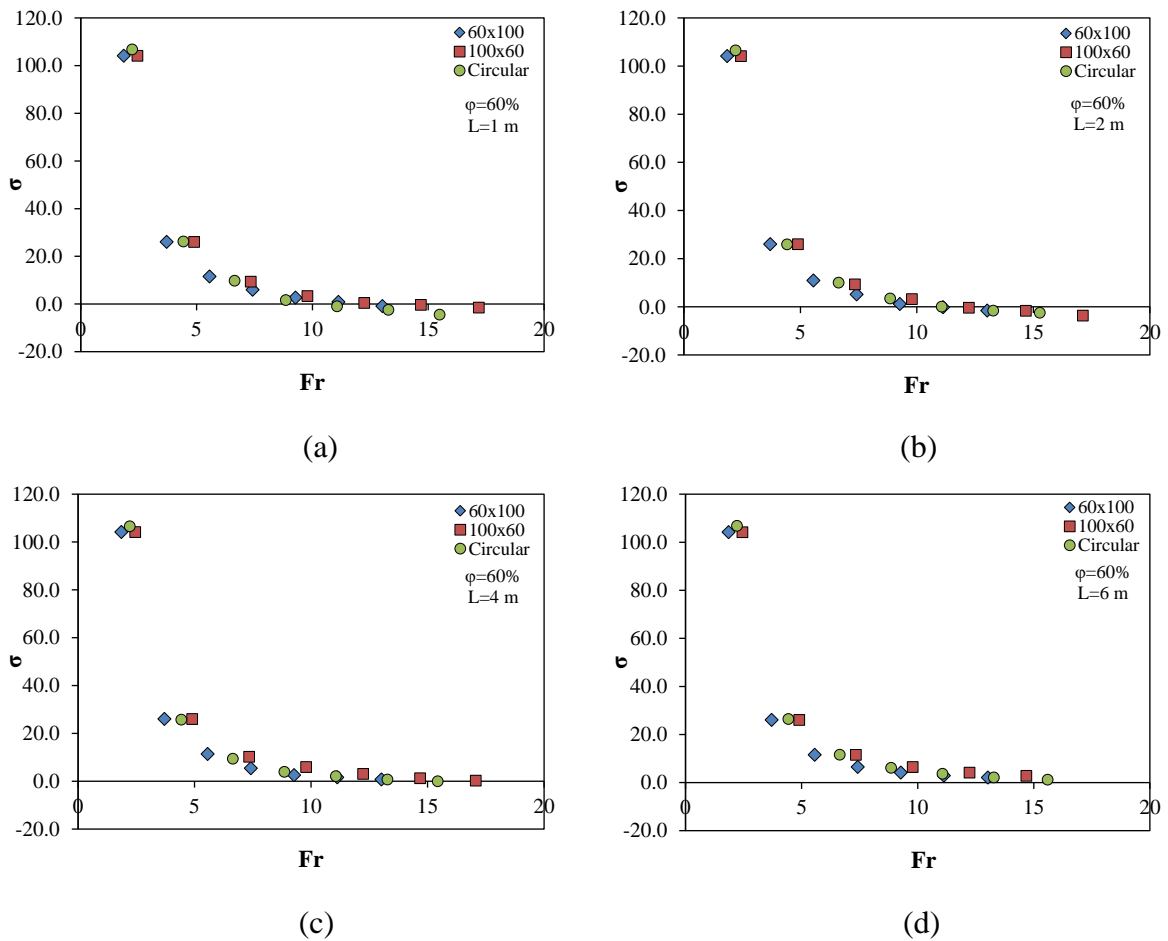
224





225 **Figure 9.** Variation of  $\sigma$  plotted against the Froude number for different bottom outlet lengths  
226 at  $\varphi=40\%$  (a)  $L=1 \text{ m}$ , (b)  $L=2 \text{ m}$ , (c)  $L=4 \text{ m}$ , (d)  $L=6 \text{ m}$

227



228 **Figure 10.** Variation of  $\sigma$  plotted against the Froude number for different bottom outlet lengths  
229 at  $\varphi=60\%$  (a)  $L=1 \text{ m}$ , (b)  $L=2 \text{ m}$ , (c)  $L=4 \text{ m}$ , (d)  $L=6 \text{ m}$

230

231

232

233 **4. Prediction Model**

234 Regression analysis was performed using the nonlinear regression module. An empirical  
235 correlation was developed to predict the cavitation index that can be used for all bottom outlet  
236 cross-sections with a sluice gate. The resulting correlation is shown in Eq. (8). For the 504 data  
237 points used, the correlation coefficient ( $R^2$ ) is 0.95. Good agreement was found between the  
238 observed and calculated cavitation index.

239

$$\sigma = 192.590 Fr^{-1.306} \varphi^{-0.536} \left( \frac{R_h}{L} \right)^{-0.029} - 11.873 \quad (8)$$

240

241 where  $\sigma$  is cavitation index,  $Fr$  is the Froude number,  $\varphi$  is gate opening rate,  $R_h$  is hydraulic  
242 radius, and  $L$  is bottom outlet length.

243

244 **5. Conclusions**

245 The present study investigates the effect of bottom outlet cross-sectional geometry, gate  
246 opening rate, bottom outlet length, and Froude number on cavitation index. The results obtained  
247 are listed below.

248 • The cavitation index decreased with increasing Froude number for all bottom outlet  
249 cross-sectional geometries, gate opening rates, and bottom outlet lengths. This indicates the  
250 presence of an inverse relationship between the Froude number and the cavitation index.

251 • Negative values for the cavitation index were observed at Froude number 25 at 10%  
252 gate opening rates, Froude number 20 at 15% gate opening rates, Froude number 15 at 20%  
253 gate opening rates, Froude number 12 at 30% gate opening rates, Froude number 10 at 40%  
254 gate opening rates, and Froude number 8 at 60% gate opening rates.

255 • As the gate opening rate increased, the cavitation index had larger values at low Froude  
256 numbers for all bottom outlet cross-sectional geometries and bottom outlet lengths. The  
257 cavitation index reached zero at lower Froude numbers as the gate opening rate increased.

258 • There was no risk of cavitation for Froude numbers less than 20 at 10% gate opening  
259 rates, values of Froude numbers less than 15 at 15% gate opening rates, values of Froude  
260 numbers less than 13 at 20% gate opening rates, values of Froude numbers less than 11 at 30%  
261 gate opening rates, values of Froude numbers less than 10 at 40% gate opening rates and values  
262 of Froude numbers less than 9 at 60% gate opening rates.

263 • The bottom outlet cross-sectional geometry did not have a big effect on the cavitation  
264 index for all gate opening rates and bottom outlet lengths.

- 265 • The effect of bottom outlet length on the cavitation index was not found to be significant  
266 for all bottom outlet cross-sectional geometries and gate opening rates.
- 267 • The equation developed in this study will be of considerable utility in estimating the  
268 cavitation index. Researchers will be able to use this equation to determine the cavitation index  
269 at the design stage without the need for experimental studies. This will provide researchers with  
270 a significant advantage in terms of time and economy.

271

## 272 **Acknowledgments**

273 The authors would like to thank The Scientific and Technological Research Council of Turkey  
274 for financially supporting the research project (Ref. No. 215M046).

275

## 276 **Data Availability Statement**

277 All data used is appended (available in the Supplementary Data section) or is included in the  
278 submitted article.

279

## 280 **Notation**

281	$D_0$	diameter of air vent.
282	Fr	Froude number based on effective depth in bottom outlet
283	g	gravitational acceleration
284	$h_a$	ambient pressure in m of water
285	$h_e$	effective depth
286	$h_p$	local water pressure in m of water
287	$h_v$	saturated water vapor pressure in m of water
288	L	length of bottom outlet
289	$L_0$	length of air vent
290	$P_a$	relative air pressure
291	$P_v$	saturated water vapor pressure
292	$R_h$	hydraulic radius
293	$Q_a$	air flow rate measured through air vent
294	$Q_a/Q_w$	air-demand ratio
295	$Q_w$	water flow rate in bottom outlet
296	$V_a$	mean air-flow velocity in air vent
297	$V_w$	mean water-flow velocity under gate
298	$\lambda$	friction coefficient

299	$\xi$	total loss coefficient of air vent
300	$\xi_{fr}$	frictional resistance coefficient of air vent length
301	$\xi_{loc}$	local fluid resistance coefficient
302	$\rho_a$	air density
303	$\sigma$	cavitation index
304	$\phi$	ratio of water cross-sectional flow area to bottom outlet cross-sectional area
305		

## 306 References

- 307 Aydin, A.B., Baylar, A., Ozkan, F., Tuna, M.C. and Ozturk, M., (2021), “Influence of cross-  
308 section geometry on air demand ratio in high-head conduits with a radial gate”, Water Supply,  
309 21 (8), 4086-4097.
- 310 Aydin, A.B., Baylar, A., Ozkan, F., Tuna, M.C. and Ozturk, M., (2024a), “Investigation of the  
311 geometry effect on air-demand ratio in conduits with a sluice gate”, Proceedings of the  
312 Institution of Civil Engineers-Water Management, 177 (4), 201-210.
- 313 Aydin, A.B., Baylar, A., Ozkan, F., Tuna, M.C. and Ozturk, M., (2024b), Role of gate type in  
314 the air-demand ratio in closed conduits”, Journal of Applied Engineering Sciences, 14 (1), 17-  
315 26.
- 316 Aydin, A.B., Tuna, M.C. and Baylar, A., (2022), “Application of gated conduits for fertigation  
317 in irrigation systems”, Water Practice and Technology, 17 (7), 1515-1522.
- 318 Baylar, A. and Batan, M., (2010), “Usage of artificial intelligence methods in free flowing gated  
319 closed conduits for estimation of oxygen transfer efficiency”, Advances in Engineering  
320 Software, 41 (5), 729-736.
- 321 Baylar, A., Ozkan, F. and Tuna, M.C., (2021), “The effect of cross-section variation of high  
322 head gated conduits on aeration performance”, Project No. 215M046, The Scientific and  
323 Technological Research Council of Turkey.
- 324 Baylar, A., Ozkan, F., Yildirim, C.B., Aydin, A.B., Tuna, M.C. and Ozturk, M., (2022), “The  
325 role of cross-sectional geometry of high-head gated conduit in oxygen transfer efficiency”,  
326 Water and Environment Journal, 36 (3), 372-379.
- 327 Baylar, A., Unsal, M. and Ozkan, F., (2010), “Hydraulic structures in water aeration processes”,  
328 Water, Air, and Soil Pollution, 210 (1), 87-100.

- 329 Campbell, F.B. and Guyton, B., (1953), "Air-demand in gated outlet works", Proceedings of  
330 the 5th IAHR Congress, Minneapolis, MN, USA, IAHR, 1-4 September, 529-533.
- 331 Chanson, H., 2000, "Aeration and deaeration at bottom aeration devices on spillways",  
332 Canadian Journal of Civil Engineering, 21 (3), 404-409.
- 333 Dong, Z.Y. and Su, P.L., (2006), "Cavitation control by aeration and its compressible  
334 characteristics", Journal of Hydrodynamics, 18 (4), 499-504.
- 335 Escarameia, M., (2007), Investigating hydraulic removal of air from water pipelines,  
336 Proceedings of the Institution of Civil Engineers-Water Management, 160 (1), 25-34.
- 337 Falvey, H.T., 1990, "Cavitation in chutes and spillways", A Water Resources Technical  
338 Publication, Engineering Monograph No. 42, US Department of the Interior, Bureau of  
339 Reclamation, Denver, CO.
- 340 Falvey, H.T., (1983), "Prevention of cavitation on chutes and spillways", In Proc., Conf. on  
341 Frontiers in Hydraulic Engineering, ASCE, 432-437, Reston, VA.
- 342 Haindl, K. and Sotornik, V., (1957), "Quantity of air drawn into a conduit by the hydraulic jump  
343 and its measurement by gamma-radiation", Proceedings of the 7th IAHR Congress, Lisbon,  
344 Portugal, IAHR, 7-9 January, D31.1-D31.7.
- 345 Hohermuth, B., (2019), "Aeration and two-phase flow characteristics of low-level outlets",  
346 Ph.D. thesis, ETH Zurich, Switzerland. doi: <https://doi.org/10.3929/ethz-b-000351715>.
- 347 Hohermuth, B., Schmocke, L. and Boes, R.M., (2020), "Air demand of low-level outlets for  
348 large dams", Journal of Hydraulic Engineering, ASCE, 146 (8), 04020055.
- 349 Kalinske, A.A. and Robertson, J.M., (1943), "Closed conduit flow", Transactions of the  
350 American Society of Civil Engineers, ASCE, 108 (1), 1435-1447.
- 351 Lee, W. and Hoopes, J.A., (1996), "Prediction of cavitation damage for spillways", Journal of  
352 Hydraulic Engineering, ASCE, 122 (9), 481-488.
- 353 Matos, J., Novakoski, C.K., Ferla, R., Marques, M.G., Dai Prá, M., Canellas, A.V.B. and  
354 Teixeira, E.D., (2022), "Extreme pressures and risk of cavitation in steeply sloping stepped  
355 spillways of large dams" Water, 14 (3), 306.
- 356 May, R.W.P., (1987), "Cavitation in hydraulic structures: Occurrence and prevention",  
357 Hydraulics Research Report, No. SR 79, Wallingford, UK.

- 358 Mortensen, J.D. and Kubitschek, J.P., (2016), “Effects of hydraulic jump motion on air  
359 entrainment in closed conduits”, 6th IAHR International Symposium on Hydraulic Structures,  
360 Portland, OR, USA, IAHR, 27-30 June, 511-518.
- 361 Mortensen, J.D., (2009), Factors affecting air entrainment of hydraulic jumps within  
362 closed conduits”, MSc Thesis, Utah State University, Logan, Utah.
- 363 Mortensen, J.D., Barfuss, S.L. and Johnson, M.C., (2011), “Scale effects of air entrained by  
364 hydraulic jumps within closed conduits”, Journal of Hydraulic Research, 49 (1), 90-95.
- 365 Mortensen, J.D., Barfuss, S.L. and Tullis, B.P., (2012), “Effects of hydraulic jump location on  
366 air entrainment in closed conduits”, Journal of Hydraulic Research, 50 (3), 298-303.
- 367 Novak, P., Moffat, A.I.B., Nalluri, C. and Narayanan, R., (2007), “Hydraulic Structures”, 4<sup>th</sup>  
368 Edition, CRC Press, London, <https://doi.org/10.1201/9781315274898>
- 369 Oveson, D.P., (2008), “Air demand in free flowing gated conduits”, MSc Thesis, Utah State  
370 University, Logan, Utah.
- 371 Ozkan, F., Baylar, A. and Ozturk, M., (2006a), “Air entrainment and oxygen transfer in high-  
372 head gated conduits”, Proceedings of the Institution of Civil Engineers-Water Management,  
373 159 (2), 139-143.
- 374 Ozkan, F., Baylar, A. and Ozturk, M., (2010), Closure of “Air entraining and oxygen transfer  
375 in high-head gated conduits”, Proceedings of the Institution of Civil Engineers-Water  
376 Management, 163 (2), 103-104.
- 377 Ozkan, F., Baylar, A. and Tugal, M., (2006b), “The performance of two phase flow systems in  
378 pond aeration”, International Journal of Science and Technology, 1 (1), 65-74.
- 379 Ozkan, F., Demirel, I.H., Tuna, M.C. and Baylar, A., (2015), “The effect of length of free-  
380 surface gated circular conduit on air-demand ratio and aeration efficiency”, Water Science and  
381 Technology: Water Supply, 15 (6), 1187-1192.
- 382 Ozkan, F., Tuna, M.C., Baylar, A. and Ozturk, M., (2014), “Optimum air-demand ratio for  
383 maximum aeration efficiency in high-head gated circular conduits”, Water Science and  
384 Technology, 70 (5), 871-877.
- 385 Pengchengi, L., David, Z.Z., Tingyu, X. and Jian, Z., (2022), “Air demand of a hydraulic jump  
386 in a closed conduit”, Journal of Hydraulic Engineering, ASCE, 148 (2), 04021058.

- 387 Sharma, H.R., (1976), "Air-entrainment in high head gated conduits", Journal of the Hydraulics  
388 Division, Proceedings of the American Society of Civil Engineers, ASCE, 102 (11), 1629-1646.
- 389 Speerli, J. and Hager, W.H., (2000), Air-water flow in bottom outlets", Canadian Journal of  
390 Civil Engineering, 27 (3), 454-462.
- 391 Speerli, J., (1999), "Air entrainment of free-surface tunnel flow", Proceedings of the 7th IAHR  
392 Congress, Graz, Austria, IAHR, 22-27 August, CD-ROM.
- 393 Stahl, H. and Hager, W.H., (1999), "Hydraulic jump in circular pipes", Canadian Journal of  
394 Civil Engineering, 26 (3), 368-373.
- 395 Tullis, B.P. and Larchar, J., (2011), "Determining air demand for small- to medium-sized  
396 embankment dam low-level outlet works", Journal of Irrigation and Drainage Engineering,  
397 ASCE, 137 (12), 793-800.
- 398 Tuna, M.C., Ozkan, F. and Baylar, A., (2014), "Experimental investigations of aeration  
399 efficiency in high head gated circular conduits", Water Science and Technology, 69 (6), 1275-  
400 1281.
- 401 U. S. Bureau of Reclamation, (1966), "Hydraulic Model Studies of the Silver Jack Outlet Works  
402 Bypass, Bostwick Park Project", USBR, Denver, Colorado.
- 403 U.S. Army Corps of Engineers, (1964), "Hydraulic Design Criteria: Air-Demand-Regulated  
404 Outlet Works", USACE, Chart 050-1.
- 405 Unsal, M., Baylar, A., Kayadelen, C. and Ozkan, F., (2014), "The modeling of oxygen transfer  
406 efficiency in gated conduits by using genetic expression programming", Journal of Engineering  
407 Research, 2 (2), 15-28.
- 408 Unsal, M., Baylar, A., Tugal, M. and Ozkan, F., (2008), "Increased aeration efficiency of high-  
409 head conduit flow systems", Journal of Hydraulic Research, 46 (5), 711-714.
- 410 Unsal, M., Baylar, A., Tugal, M. and Ozkan, F., (2009), "Aeration efficiency of free-surface  
411 conduit flow systems", Environmental Technology, 30 (14), 1539-1546.
- 412 Wahl, T.L. and Falvey, H.T., (2022), "SpillwayPro: Integrated water surface profile, cavitation,  
413 and aerated flow analysis for smooth and stepped chutes", Water, 14 (8), 1256.
- 414 Wahl, T.L., Frizell, K.W. and Falvey, H.T., (2019), "SpillwayPro-Tools for analysis of spillway  
415 cavitation and design of chute aerators", Hydraulic Laboratory Report HL-2019-03, Bureau of  
416 Reclamation, Denver, CO.

- 417 Wisner, P., (1965), "On the role of the Froude criterion for the study of air entrainment in high  
418 velocity flows", Proceedings of the 11th IAHR Congress, Leningrad, USSR, IAHR, 6-11  
419 September, Paper 1.15.
- 420 Wisner, P., (1967), "Air entrainment in high speed flows", Proceedings of the 9th ICOLD  
421 Congress, Istanbul, Turkey, 4. - 8. September, 495-507.